NATIONAL ADVISORY COMMITTEE FOR AERONAUTICS

TECHNICAL NOTE 3265

VAPORIZATION RATES AND DRAG COEFFICIENTS FOR ISOOCTANE SPRAYS IN TURBULENT AIR STREAMS

By Robert D. Ingebo

Lewis Flight Propulsion Laboratory
Cleveland, Ohio

Washington
October 1954

NATIONAL ADVISORY COMMITTEE FOR AERONAUTICS

TECHNICAL NOTE 3265

VAPORIZATION RATES AND DRAG COEFFICIENTS FOR ISOOCTANE SPRAYS IN TURBULENT AIR STREAMS

By Robert D. Ingebo

SUMMARY

A droplet camera developed at the NACA Lewis laboratory was used to obtain drop-size distribution and drop-velocity data for isooctane injected from a simple orifice directly into a turbulent air stream. From these data and wet-bulb temperature data, vaporization rates and drag coefficients were calculated for isooctane drops accelerating and evaporating in streams having velocities of 140 and 180 feet per second. Spray vaporization rates based on the mean drop diameter D_{20} were compared with single-drop vaporization rates by use of the heat-transfer equation

$$\frac{dD_{20}^2}{d\theta} = \frac{4k_g \Delta t}{\rho_L H_v} Nu_{20}$$

where D_{20} is defined as the diameter of a drop having an area equal to the ratio of total area to total number of drops formed in the spray, θ is the time, k_g is the thermal conductivity of the air, Δt is the difference between the air temperature and drop-surface (wet-bulb) temperature, ρ_L is the density of the liquid, H_v is the latent heat of vaporization, and Nu_{20} is the heat-transfer Nusselt number based on the mean drop diameter D_{20}. For these tests, the change in sensible heat of the liquid was negligible compared with latent heat requirements. The weight percent of the spray evaporated at distances of 1 to 18 inches downstream of the injector was determined and found to be in agreement with data obtained in a previous investigation by means of a sampling-probe technique.

Nukiyama-Tanasawa and log-probability drop-size-distribution functions gave good agreement with experimental drop-size-distribution data in the determination of mean drop size. The Sauter mean diameter for the spray, predicted by the Nukiyama-Tanasawa empirical expression for a

different type of nozzle, agreed with that found for the 180-feet-per-second air stream. The maximum drop diameter for the isooctane sprays was calculated from a balance of aerodynamic pressure and surface tension forces under the condition of maximum acceleration of the sprays. These values compared well with the maximum drop diameter observed from photomicrographs of the sprays.

INTRODUCTION

When a liquid fuel is injected into the preignition zone of a ram jet or a turbojet engine, or into an afterburner, the liquid is broken up into a cloud of droplets which are then accelerated to stream velocity. While accelerating, they evaporate at a rate determined by: (1) the air-stream velocity, temperature, and static pressure, (2) the droplet velocity, temperature, and diameter, and (3) the physical properties of the liquid and vapor. Thus, the vaporization rate of sprays in air streams of known temperature, pressure, and velocity may be determined by use of heat-transfer equations when data on drop-size distribution, drop acceleration, and drop-surface temperature are available.

Several investigators (e.g., refs. 1 and 2) have obtained drop-size-distribution data for the atomization of liquids in air streams. However, the problem of correlating drop-size-distribution parameters with physical characteristics of the atomization process is still unsolved. Data have been obtained (refs. 3 and 4) for the weight percent of fuel spray evaporated in air streams at given distances downstream of the injector by means of a sampling technique. Since this method did not give data on drop size and drop velocity, a correlation with characteristics of momentum, mass, and heat transfer could not be made. Correlations of this type have been made for single drops evaporating in air streams (refs. 5 and 6). However, the problem of relating vaporization rates of single drops to that of sprays has not been solved because of the lack of spray vaporization-rate data.

In reference 7, theoretical equations are given for predicting the vaporization rate of fuel spray based on a single mean-diameter droplet. For simplicity, an evaporation constant, assumed to be independent of drop size and velocity, was used. An expression valid only for either exceedingly fine sprays or sprays which have accelerated to stream velocity was obtained. If the doubtful assumption is made that evaporation prior to obtaining either of these conditions is negligible, the equation of reference 7 may be applied directly to the evaporation of fuel sprays in jet engines.

In this investigation, data on drop-size distribution, drop velocity, and drop-surface (wet-bulb) temperature were obtained for isooctane sprays in turbulent air streams having velocities of 140 and 180 feet per second. This was accomplished by using a droplet camera developed

at the NACA Lewis laboratory which gave photomicrographs of the sprays and also drop-velocity data. Drop-size-distribution data were obtained from photomicrographs of the spray; and the wet-bulb temperature for isooctane, under the conditions of this investigation, was obtained by the experimental technique described in references 5 and 6. From these data, it was possible to calculate the following spray parameters: (1) mean-drop sizes, (2) vaporization rates, (3) drag coefficients, and (4) weight percent evaporated.

SYMBOLS

The following symbols are used in this report:

A	surface area of drop, sq cm
A'	frontal area of drop, sq cm
a	acceleration of drop, ft/sec^2
b	constant
$b_{g,w}$	molecular mass diffusivity, g/(cm)(sec)
C_D	drag coefficient
$\bar{c}$	root-mean-square velocity of air molecules, cm/sec
D	drop diameter, cm
ΔD	drop-diameter size range, cm
$\bar{D}$	constant
D_{20}, D_{30}, D_{31}, D_{32}	mean drop diameter defined by the expression $D_{j-k} = \frac{\Sigma nD^j}{\Sigma nD^k}$, for example, D_{20} is the diameter of a single drop having an area equal to the total area to number ratio for all the drops formed in a spray, cm
E	portion of total spray which has evaporated, percent
F	total force of air stream, dynes
G	momentum
g	acceleration due to gravity, 980 cm/sec^2

H_v	latent heat of vaporization, g-cal/g
h	heat-transfer coefficient, g-cal/(sec)(sq cm)(^oC)
k	thermal conductivity, g-cal/(sec)(sq cm)(^oC)/cm)
L	distance from mirror to film, ft
l	mean free path of air molecules, cm
M	magnification factor for lens system, 2l power
m	mass of liquid, g
$dm/d\theta$	vaporization rate, g/sec
Δm	mass of liquid vaporized, g
Nu	heat-transfer Nusselt number, hD/k
Nu_{20}	heat-transfer Nusselt number based on mean drop diameter D_{20}, hD_{20}/k
n	number of drops in given size range
p_a	air-stream static pressure, in. Hg abs
p_L	fuel injection pressure drop, lb/sq in.
Q	volumetric flow rate, cc/sec
q	constant
R	volume fraction of drops having diameter > D
Re	Reynolds number based on drop diameter, $D\Delta u\rho/\mu$
T	temperature, ^oR
t	temperature, ^oC
Δt	difference between air temperature and surface temperature of drop, $t_s - t_d$, ^oC
U	velocity, ft/sec

Δu	relative velocity of air with respect to drop, cm/sec
v	volume fraction of drops having diameter < D
We_c	critical Weber number, $\rho_a U_s^2 D_m / 2\sigma$
x	distance downstream from the injector orifice, in.
y	$\ln(D/\overline{D})$
δ	constant
θ	vaporization time, sec
λ	evaporation constant, $4k_g \Delta t / p_L H_v$, sq cm/sec
μ	fluid viscosity, poises
ρ	fluid density, g/cu cm
σ	surface tension, dynes/cm
ω	mirror speed, rpm

Subscripts:

a	air
d	drop
f	final condition
g	gas
i	initial condition
L	liquid
m	maximum
s	air stream
v	vapor

APPARATUS AND PROCEDURE

The vaporization rates of isooctane sprays evaporating and accelerating in turbulent air streams were determined experimentally with the apparatus shown in figure 1. Air at $82^{\circ}\pm3^{\circ}$ F and 16±1 percent relative humidity was supplied from the central laboratory system at 40 pounds per square inch gage. The air was metered with a variable-area orifice and exhausted to the altitude exhaust system. In order to minimize approach-stream turbulence, a 30 by 28 mesh, 0.013-inch-diameter monel wire screen was placed 5 feet 4 inches upstream of the inlet to the transparent 8-inch-inside-diameter plastic test section. Two transparent 2- by 2- by 3/8-inch optically flat plastic windows were installed in the test section for photographing the spray. Air-stream pressure and velocity in the test section were controlled by upstream and downstream valves.

Isooctane fuel (2, 2, 4-trimethylpentane, A.S.T.M. specifications) was injected by pressurized nitrogen into the test section through a 1/4-inch-diameter Inconel tube sealed at the end. A 0.041-inch-diameter orifice was drilled and reamed to size 1 inch from the sealed end in order to obtain a smooth surface. The orifice was pointed directly into the air stream and positioned on the test-section center line (position 4, fig. 1) and also moved vertically to positions 1, 2, 6, and 7 in figure 1 so that photomicrographs could be obtained over a vertical transverse of the spray cross section.

Drop-size and drop-velocity data were obtained by photographing the spray at distances of 1, $5\frac{1}{2}$, 14, and 18 inches downstream of the fuel injector center line. A camera unit developed at the NACA Lewis laboratory (ref. 8) was positioned at the 2-inch-square plastic windows, as shown in figure 1, to obtain photomicrographs of the isooctane spray in natural suspension in the high-velocity air stream. The object plane was centered along the test section center line (position 4, fig. 1) and also moved horizontally to obtain a horizontal traverse of the spray cross section (positions 3 and 5, fig. 1). Thus, by adjusting the camera unit in a horizontal direction and the fuel injector in a vertical direction, a seven-position traverse was made of the spray cross section at each of the four distances downstream of the injector.

The lens system used in the camera unit had a magnification factor of 21, a 1-centimeter-square field area, a field depth of 1 millimeter, and resolved droplets as small as 5 microns in diameter. Stopped images of the high-velocity droplets were obtained on the film, as shown in figure 2, by means of the rotating mirror and synchronized flash system shown in figure 1.

The original droplet camera described in reference 1 was modified considerably in this investigation, since the additional factors of high droplet concentrations and varying droplet velocity were considered. The three-phase 400-cycle inverter was rewired and a rheostat was connected in the field circuit so that the speed of the rotating mirror could be varied from 3,000 to 11,000 rpm. The pair of 0.05-microfarad condensers were replaced with a pair of 1.0-microfarad condensers which gave a higher intensity flash when discharged across the two 0.014- by 0.1-inch magnesium-ribbon electrodes spaced 3/8 inch apart and sandwiched between split cylinders of bakelite insulation. Also, the lens system was redesigned and a modified aerial camera with the shutter and lens removed was used primarily as a holder for the 9.5-inch-width roll film.

By using 1.0-microfarad condensers, which gave a very brilliant flash, it was possible to test various fuel dyes, light filters, film types, and developing solutions for obtaining high-contrast negatives. Best results were obtained with a clear fuel (not dyed), a Wratten red filter No. 25 mounted on the light source, and a shellburst panchromatic-type film developed with a D-11 solution. The red light, because of its relatively long wave length, gave a minimum of light scattering in the spray, and thus sharp droplet images were obtained on the high-contrast shellburst film. The D-11 solution was a standard developer generally used for high-contrast work.

The following procedure was used in obtaining photomicrographs of the spray: The air velocity in the test section was set at 140 or 180 feet per second. An air temperature of $82^{\circ}\pm3^{\circ}$ F and static pressure of 29.3±0.3 inches of mercury were used in both cases. Isooctane metered at a flow rate of 100 pounds per hour with a rotameter was injected from the contrastream orifice into the air stream with a pressure drop of 55 pounds per square inch across the orifice. Photomicrographs of the spray were then taken over a range of mirror speeds. From the photomicrographs, the correct mirror speed required for obtaining stopped-droplet images on the film and also droplet velocity was determined. Photomicrographs of the spray were taken at the proper mirror speed and analyzed to obtain drop-size-distribution data. An average of seven pictures were obtained at each of the seven points in the traverse of the spray cross section, and all the droplets in focus and stopped on the film were measured to obtain at least 1400 droplets for each analysis. The same procedure was repeated at distances of 1, $5\frac{1}{2}$, 14, and 18 inches downstream of the injector to obtain vaporization-rate data.

Measurements of droplet diameters were made from the photomicrographs with an eyepiece having small-scale subdivisions of 0.10 millimeter which gave droplet diameters accurate within ±3 microns. The camera was calibrated with a Bausch and Lomb microscope slide having

small-scale subdivisions of 10 microns. Since 1400 to 1800 drops were measured for each analysis of the spray cross section, a statistical error factor of approximately $3\frac{1}{2}$ percent was calculated for each cummulative distribution analysis.

The wet-bulb temperature for isooctane droplets evaporating under the conditions of this investigation was obtained experimentally. From the data on drop diameter, velocity, and wet-bulb temperature, it was possible to calculate vaporization rates and drag coefficients for the isooctane sprays.

RESULTS AND ANALYSIS

The following steps were employed in the analysis of the data:

(1) A spray-vaporization-rate equation based on the mean drop diameter D_{20} was written for the case of simultaneous acceleration and evaporation of sprays.

(2) Drop-size-distribution data, obtained from photomicrographs, were used to calculate the mean drop size D_{20} for each spray analysis.

(3) Drop velocities were calculated and used to determine vaporization times and droplet drag coefficients.

(4) A comparison was made between the predicted and observed maximum droplet diameter in the spray.

(5) Spray vaporization rates based on mean drop diameter D_{20} were compared with values predicted by single-drop vaporization-rate equations (refs. 5 and 6).

(6) The weight percent of the spray evaporated at distances of 1, $5\frac{1}{2}$, 14, and 18 inches downstream of the injector was determined and compared with values predicted by an empirical expression (ref. 4).

Vaporization-Rate Equations

The instantaneous vaporization rate $dm/d\theta$ of a drop may be determined from the heat-transfer equation

$$\frac{dm}{d\theta} H_v = hA\Delta t = \pi D k_g \Delta t Nu \qquad (1)$$

when the change in sensible heat of the liquid is negligible compared with latent heat requirements. In recent investigations (refs. 5 and 6), the following expression was obtained for the heat-transfer Nusselt number:

$$Nu = \frac{hD}{k_g} = 2 + 2.58 \times 10^6 \left(\frac{\rho \Delta u D}{b_{g,w}} \frac{gl}{c^2}\right)^{0.6} \left(\frac{k_g}{k_v}\right)^{0.5} \tag{2}$$

where the product of the Reynolds and Schmidt numbers is given as a single dimensionless number equal to $\rho \Delta u D / b_{g,w}$, and the momentum-transfer ratio gl/c^2 is the ratio of gravitational to viscous forces.

Equation (1) may be rewritten by expressing the instantaneous vaporization rate in terms of the change in drop area with time and solving for the Nusselt number as follows:

CA-2

$$Nu = \frac{\rho_L H_v}{4 k_g \Delta t} \frac{dD^2}{d\theta} \tag{3}$$

where Nu is the heat-transfer Nusselt number for a single drop.

The change in area of the spray A may be written as the sum of (1) the area of the completely evaporated drops, and (2) the change in area of the partially evaporated drops:

$$\Delta A = \pi \sum_{D=0}^{D=\sqrt{\lambda \Delta \theta Nu}} n D^2 + \pi \lambda \Delta \theta \sum_{D=\sqrt{\lambda \Delta \theta Nu}}^{D=D_m} n\, Nu \tag{4}$$

where $\lambda = 4 k_g \Delta t / \rho_L H_v$. During each experimental time increment $\Delta \theta$, the decrease in spray area due to complete evaporation of small drops was negligible (approximately 1 percent) compared with the decrease in area due to partial evaporation of the larger drops in the sprays. Thus, the above expression was rewritten as

$$\frac{\Delta A}{\Delta \theta} = \pi \lambda \sum_{D=0}^{D=D_m} n\, Nu \tag{5}$$

For this investigation, equation (2) may be written

$$Nu = 2 + 0.39\, Re^{0.6}$$

(since $b_{g,w} = 2.7 \times 10^{-4}$ g/(cm)(sec), $gl/c^2 = 1.024 \times 10^{-12}$, and $(k_a/k_v)^{0.5} = 1.64$.) By combining equations (4) and (5) and dividing each side of the resulting equation by $\sum_{D=0}^{D=D_m} n$, the expression

$$\frac{\Delta D_{20}^2}{\Delta\theta} = \lambda\left[2 + 0.39\left(\frac{\Delta u \rho_a}{\mu_a}\right)^{0.6}\sum_{D=0}^{D=D_m} nD^{0.6}\Big/\sum_{D=0}^{D=D_m} n\right] \tag{6}$$

is obtained, where $D_{20}^2 = \Sigma nD^2/\Sigma n$. It was found experimentally that:

$$\frac{\sum_{D=0}^{D=D_m} nD^{0.6}\Big/\sum_{D=0}^{D=D_m} n}{D_{20}^{0.6}} = 0.90 \pm 0.02 \tag{7}$$

Thus, combining this expression with equation (6) and passing to the limit yields

$$\frac{dD_{20}^2}{d\theta} = \lambda\left[2 + 0.35\left(\frac{D_{20}\Delta u \rho_a}{\mu_a}\right)^{0.6}\right] = \frac{4k_g\Delta t}{\rho_L H_v} Nu_{20} \tag{8}$$

where the term in brackets represents the Nusselt number based on the mean drop diameter D_{20}.

The mean Nusselt number Nu_{20} may be determined from equation (8) and compared with the single-drop Nusselt number given by equation (2) when the spray parameters dD_{20}^2, Δu, and Δt are known. Since the surface temperature of each drop could not be determined experimentally, the wet-bulb temperature of isooctane was obtained experimentally and assumed equal to the surface temperature of a single drop having a mean drop diameter equal to D_{20}. The remaining parameters dD_{20}^2 and Δu were determined experimentally.

Drop-Size-Distribution Analyses

Determination of mean drop sizes. - Analyses of the drop-size distribution for isooctane sprays at distances of 1, $5\frac{1}{2}$, 14, and 18 inches downstream of the fuel injection station were made for air-stream velocities of 140 and 180 feet per second. Table I shows the drop-size count obtained at each of the seven positions in the spray cross-section traverse for a representative test. A complete traverse of the positions 1 to 7 and total drop-size count are included in this table. Eight total-drop-size counts are recorded in table II, and a typical plot of drop-size distribution is shown in figure 3.

Three of the most common mathematical expressions for drop-size distribution are the Rosin-Rammler, Nukiyama-Tanasawa, and log-probability equations. A description of the evaluation and use of these expressions is given in reference 9. They may be written as follows:

Rosin-Rammler,

$$\frac{dR}{dD} = \frac{-qD^{q-1}}{\overline{D}^{q}} e^{-(D/\overline{D})^{q}} \tag{9}$$

Nukiyama-Tanasawa,

$$\frac{dR}{dD} = -\frac{b^{6}}{120} D^{5} e^{-bD} \tag{10}$$

log-probability,

$$\frac{dv}{dy} = \frac{\delta}{\sqrt{\pi}} e^{-\delta^{2}y^{2}} \tag{11}$$

Drop-size-distribution data were plotted for each of the eight analyses using each of the three distribution equations. Samples of these plots are shown in figures 4 to 6. The Nukiyama-Tanasawa and log-probability expressions gave good agreement with values of D_{20} obtained by direct integration of the data. Results for the test condition $U_s = 140$ feet per second and $x = 5.5$ inches are shown in the following table:

Mathematical expression	Mean drop diameter, D_{20}, microns
Rosin-Rammler	21.1
Nukiyama-Tanasawa	41.3
Log-probability	40.7
Direct integration	41.3

The Rosin-Rammler expression gave poor agreement since q in equation (9) was found to be approximately equal to 3. When q is equal to 3 in this expression, number mean diameters such as D_{20} are predicted to be equal to zero. This, of course, limits the usefulness of equation (9). A similar limitation of the Rosin-Rammler equation was found in reference 9.

Comparison with predicted mean drop sizes. - Reference 10 gives the following empirical expression for predicting the Sauter mean diameter D_{32} produced by a gas atomizing nozzle:

$$D_{32} = \frac{1920}{U_s}\sqrt{\frac{\sigma}{\rho_L}} + 597\left(\frac{\mu_L}{\sigma\rho_L}\right)^{0.45}\left(\frac{1000Q_L}{Q_s}\right)^{1.5} \tag{12}$$

For this investigation, Q_L/Q_s is small, and the expression reduces to

$$D_{32} = \frac{1920}{U_s}\sqrt{\frac{\sigma}{\rho_L}} = \frac{10,516}{U_s} \tag{13}$$

for isooctane. By using the Nukiyama-Tanasawa size-distribution expression, D_{32} may be related to D_{20} as follows (ref. 11):

$$D_{20} = 0.693\ D_{32}$$

which may be substituted into equation (13) to give

$$D_{20} = \frac{7288}{U_s} \tag{14}$$

Values for the mean drop size D_{20} obtained 1 inch downstream of the injector for the two air-stream velocity conditions are listed in the following table, with values obtained from equation (14) for comparison:

Air-stream velocity, U_s, ft/sec	Mean drop size, D_{20}, microns	
	Experimental	From eq. (14)
180	40.7	40.5
140	45.0	52.1

The agreement is good at the higher air-stream velocity. However, the effect of U_s on D_{20} appears to be greater for the calculated values shown in the preceding table. This may be because of the different type of nozzle used in the Nukiyama-Tanasawa atomization studies. It is, therefore, doubtful that the Nukiyama-Tanasawa equations can be used to predict initial drop size over wide ranges of operating conditions with the simple orifice injector used in this investigation.

Analysis of Drop-Velocity Data

Calculation of drop velocity. - The velocity of droplets which appeared on the photomicrographs as stopped images was calculated from the expression

$$U_d = \frac{4\pi L\omega}{M} \tag{15}$$

Sharply defined droplet images were obtained on the film when mirror-speed settings gave values of drop velocities calculated by the preceding expression within ±5 feet per second of the actual drop velocity. Since the duration of the magnesium flash was 4 microseconds, a droplet travel of 6 microns was permissible and droplet images on the film could be measured within ±3 microns. Droplet images were badly smeared and lacked sufficient contrast for measuring when mirror-speed settings gave drop velocities which were not within ±5 feet per second of the drop velocity.

The proper mirror speed was determined by taking photographs at a low mirror speed and gradually increasing the speed until stopped droplet images were obtained. The photographs showed that droplets of all sizes (table I) were moving at approximately the same velocity, because droplets of all sizes were stopped at a particular value of mirror speed. It was also established experimentally that a range of mirror speeds could be used in which photomicrographs were obtained showing stopped images of drops of all sizes at each of the mirror speeds. The range of mirror speeds resulting in definition of the drops was greatest at the station 1 inch downstream of the fuel injector; at this location the range of mirror speeds giving drop definition was about 20 percent of the mean value. Approximately the same drop-size distribution and mean drop size were obtained from the highest and the lowest mirror speeds giving drop definition. This range of mirror speeds was probably due to the liquid jets penetrating several inches into the air stream and being broken up into drops in the penetration zone shown in figure 7. Thus, droplets formed at the maximum point of penetration had time to accelerate to a relatively high velocity, compared with drops formed at the orifice, before reaching the camera station. Images of droplets of all sizes could be stopped at a particular value of mirror speed with the injector at each of the different locations.

Minimum mirror speeds which gave stopped droplet images were used in obtaining photomicrographs for each spray analysis so that the injector orifice could be considered to be the point of initial formation and acceleration of the spray. Drop velocities are plotted against the distance downstream from the fuel-injector orifice in figure 8 for the droplets starting at zero initial velocity at the injector orifice. For the case of solids injected into the 180-foot-per-second air stream, a 5-micron-diameter sphere would accelerate to approximately stream velocity while traveling a distance of 1 inch, whereas 5-micron drops were found to have a minimum velocity of 85 feet per second, as shown in figure 8. Thus, the acceleration of small drops was found to be considerably lower than that predicted for small solid spheres.

Calculation of vaporization time. - Vaporization time was calculated by first determining an empirical relation between drop acceleration and velocity difference, and then integrating the expression in two successive steps to obtain an equation giving distance of droplet travel

as a function of stream velocity and time. Acceleration was determined from a plot of drop velocity squared against distance (fig. 9) and the acceleration equation

$$a = \frac{U_{d,f}^2 - U_{d,i}^2}{2x}$$

Thus, the acceleration at any distance x was equal to one-half the slope of the curve in figure 9.

In order to determine a relation between drop acceleration and velocity difference, the plot shown in figure 10 was prepared. From this plot, the following empirical expression was obtained:

$$a = 333 (U_s - U_d) \tag{16}$$

Since acceleration may be expressed as the change in drop velocity with time $dU_d/d\theta$, the preceding expression may be written as

$$\int_0^{U_d} \frac{dU_d}{U_s - U_d} = 333 \int_0^{\theta} d\theta$$

Integrating between the limits shown gives

$$U_d = U_s (1 - e^{-333\theta}) \tag{17}$$

By substituting $dx/d\theta$ for droplet velocity in the preceding expression,

$$\int_0^x dx = U_s \int_0^{\theta} d\theta - U_s \int_0^{\theta} e^{-333\theta} \, d\theta$$

is obtained.

Integrating gives the final expression

$$x = U_s \left(\theta - \frac{1 - e^{-333\theta}}{333} \right) \tag{18}$$

where the vaporization time θ is an implicit function of the stream velocity U_s and the distance x.

Calculation of drop drag coefficients. - The following force balance for an evaporating droplet accelerating in an air stream was derived (appendix A):

$$F = ma + \Delta u \, dm/d\theta \tag{19}$$

The instantaneous aerodynamic pressure force of the air stream accelerating the vaporizing drop may be expressed as

$$F = \frac{1}{2} \rho_g A' (\Delta u)^2 C_D \tag{20}$$

The following equation for the drop drag coefficient was obtained by combining equations (19) and (20) and substituting into the expression terms for drop volume, drop frontal area, and vaporization rate (given by eq. (12)):

$$C_D = \frac{4}{3} \frac{\rho_L}{\rho_g} \frac{Da}{(\Delta u)^2} + \frac{8 k_g \Delta t Nu}{H_v \rho_g D \Delta u} \tag{21}$$

(For this investigation, $\rho_L = 0.69$ g/cu cm, $\rho_g = 12 \times 10^{-4}$ g/cu cm, $k_g = 5.9 \times 10^{-5}$ g-cal/(cm)(sec)($^\circ$C), $\Delta t = 25^\circ$ C, and $H_v = 73$ g-cal/g.) Drop drag coefficients were calculated from the preceding expression and plotted against the drop Reynolds number as shown in figure 11 for five velocity differences. This figure shows that the droplet drag coefficient for evaporating liquids cannot be correlated directly with the Reynolds number to obtain a single curve for all velocity differences. Drag-coefficient values for solid spheres in air streams (ref. 12) are also plotted in figure 11.

An empirical expression was obtained for the drop drag coefficient by combining equations (16) and (21) to give

$$C_D = 444 \frac{\rho_L}{\rho_a} \frac{D}{\Delta u} + \frac{8 k_g \Delta t Nu}{H_v \rho_g D \Delta u} \tag{22}$$

where the constant 444 contains the units reciprocal seconds required to balance the equation dimensionally. Further tests on the acceleration of drops are needed using other liquids and varying air-stream pressure and temperature conditions in order to establish a more general expression.

Comparison of predicted and observed maximum droplet diameters. - When the aerodynamic forces over an accelerating drop exceed the surface tension forces, the drop will shatter. Thus, it is possible to calculate the maximum drop diameter that will be found in a spray under the

condition of maximum acceleration at the injector orifice. Some investigators (refs. 13 and 14) have studied the break-up of water drops, and equated aerodynamic pressure forces and surface tension forces as follows:

$$C_D \frac{1}{2} \rho_g (\Delta u)^2 A' = \pi D \sigma$$

where A' and D are the maximum drop frontal area and diameter, respectively. Maximum drop diameters, calculated from this expression, are compared with observed values in the following table, which also shows values of the critical Weber number ($We_c = \rho a U_s^2 D_m / 2\sigma$):

Air-stream velocity, U_s, ft/sec	Maximum drop diameter, D_m, microns		Critical Weber number, We_c, based on observed D_m
	Calculated	Observed	
140	127	126	6.7
180	108	112	9.6

Thus, agreement was obtained between values of D_m calculated for atomization at the orifice and observed values obtained 1 inch downstream of the orifice.

Fuel-Spray-Evaporation Calculations

Comparison of fuel-spray and single-droplet vaporization rates. - From the drop-size distribution, drop velocity, and wet-bulb data, the instantaneous vaporization rate of the spray expressed as the change in area of the mean drop size D_{20} with time may be obtained by plotting D_{20}^2 against θ, as shown in figure 12. In order to compare single-droplet vaporization-rate equations with experimental spray vaporization rates, equations (2) and (3) were used to calculate $dD_{20}^2/d\theta$ for a single droplet, and the results were plotted in figure 12. Experimental and predicted values of D_{20} agree within approximately ±5 percent. Thus, the assumption that the mean surface temperature is closely approximated by the wet-bulb temperature appears valid in this investigation. This validity was possibly a result of low over-all fuel-vapor concentration. Although the concentration of drops was high near the injector orifice, the velocity difference Δu was also very high (droplet film thicknesses were small) so the spray evaporated essentially as a cloud of isolated droplets. Simplified vaporization-rate equations are derived in appendix B.

Comparison of predicted and experimental weight percent of spray evaporated. - Since the change in spray mass due to the complete evaporation of small drops was negligible compared with the change in mass due to the partial evaporation of larger drops in the spray, the weight percent of the spray evaporated E was calculated from the expression

$$E = 100 \frac{(D_{30}^3)_i - (D_{30}^3)_f}{(D_{30}^3)_i}$$

Values of D_{30}^3, obtained by direct integration of the drop-size-distribution data, are given in table III with the weight percent of the spray evaporated. Initial values of D_{20} were obtained from the curve in figure 12 at $\theta = 0$. Using these values, initial values of D_{30} were determined from the expression

$$D_{30} = 1.10\, D_{20} \tag{23}$$

Experimental data showed the ratio D_{30}/D_{20} was equal to 1.10±0.02, and the Nukiyama-Tanasawa expression for mean drop sizes gives

$$D_{30} = 1.13\, D_{20}$$

Table III also gives values for the weight percent of spray evaporated as calculated from the following empirical expression derived in reference 4:

$$\frac{E}{100 - E} = 9.35 \left(\frac{T_s}{1000}\right)^{4.4} \left(\frac{U_s}{100}\right)^{0.80} p_s^{-1.2}\, p_L^{0.42}\, x^{0.84} \tag{24}$$

The agreement is good except for the station 1 inch downstream of the fuel injector, which represents an extrapolation of equation (24), since the sampling probe technique could not be used for distances of less than 5 inches from the fuel injector.

SUMMARY OF RESULTS

A droplet camera was used to obtain drop-size distribution and drop-velocity data for isooctane sprays. An analysis of heat-transfer and drag data for the sprays evaporating and accelerating in turbulent air streams gave the following results:

1. Mean drop sizes were determined by direct integration of the data and compared with values obtained from an analysis of the data using the Rosin-Rammler, Nukiyama-Tanasawa, and log-probability expressions for drop-size distribution. Agreement was obtained with the Nukiyama-Tanasawa and log-probability expressions.

2. The mean drop diameter D_{20} predicted by the empirical Nukiyama-Tanasawa expression for a different type of nozzle agreed with the experimental value of D_{20} obtained at a distance of 1 inch downstream of the injector in a 180-foot-per-second velocity air stream. The effect of stream velocity on drop size predicted in the Nukiyama-Tanasawa expression is different, however, from that obtained experimentally.

3. An empirical expression was derived for the drag coefficients of isooctane drops accelerating and evaporating in turbulent air streams.

4. An expression, obtained by equating aerodynamic pressure forces and surface-tension forces for drops, was used to calculate the maximum drop size existing in the spray for the condition of maximum spray acceleration. Photomicrographs gave maximum drop diameters which were in agreement with this expression.

5. The vaporization rate of an isooctane spray based on the mean drop diameter D_{20} (defined as a drop having an area equal to the total area to total number ratio for all the drops in the spray) was found to correlate single-drop vaporization rates. The weight percent of the spray evaporated downstream of the injector was determined and found to agree with values obtained using a different technique.

CONCLUDING REMARKS

Spray-vaporization-rate data obtained in this investigation correlate single-droplet vaporization rates. The Reynolds number effect during spray acceleration was found to be very important in determining the time required to evaporate the spray. Approximately 50 percent by weight was evaporated during the acceleration period. Thus, when more data on spray acceleration and atomization are available, the expressions used in this investigation may be tested and extended in the field of spray atomization, acceleration, and evaporation.

Lewis Flight Propulsion Laboratory
National Advisory Committee for Aeronautics
Cleveland, Ohio, July 30, 1954

APPENDIX A

CHANGE OF MOMENTUM OF EVAPORATING DROP

A mass $m + \Delta m$ is considered to be moving at a velocity U_d as shown for condition I:

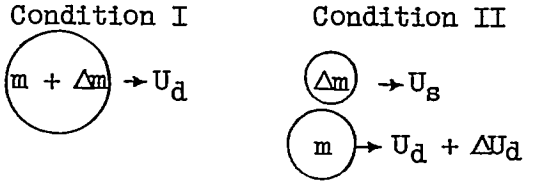

The velocity of the mass m is increased to $U_d + \Delta U_d$, and the velocity of the element Δm is increased to stream velocity U_s, as shown above for condition II. Thus, the change in momentum ΔG is given as follows:

$$\Delta G = m\,(U_d + \Delta U_d) + \Delta m\, U_s - (m + \Delta m)\, U_d$$

which reduces to

$$\Delta G = m\Delta U_d + \Delta m(U_s - U_d)$$

Dividing by $\Delta\theta$ and passing to the limit yields the instantaneous force F as follows:

$$F = \frac{dG}{d\theta} = m\,\frac{dU_d}{d\theta} + (U_s - U_d)\,\frac{dm}{d\theta}$$

where $dm/d\theta$ is the instantaneous vaporization rate.

APPENDIX B

FUEL-SPRAY-EVAPORATION CALCULATIONS

The time required to evaporate a spray may be divided into two periods: (1) the period required to accelerate the spray to approximately stream velocity, and (2) the remaining period of evaporation in which the spray travels at approximately stream velocity. In this investigation, the spray acceleration period was studied, and the spray vaporization rate (based on the mean drop diameter D_{20}) was found to agree with equation (8):

$$\frac{dD_{20}^2}{d\theta} = \frac{4k_g \Delta t}{\rho_2 H_v}\left[2 + 0.35\left(\frac{D_{20}\Delta u \rho_a}{\mu_a}\right)^{0.6}\right]$$

The final period of spray evaporation has been treated in reference 7 for the spray traveling at approximately stream velocity. Thus, a complete analysis of fuel spray evaporation may be made by treating each period separately and combining the results.

Evaporation During Spray Acceleration Period

Determination of change in D_{20}^2 during spray acceleration period. - For this investigation,

k_g, g-cal/(sec)(sq cm)($^\circ$C/cm)	5.9×10^{-5}
Δt, $^\circ$C	25
ρ_L, g/cu cm	0.69
H_v, g-cal/g	73

and the vaporization-rate equation may be written as

$$\frac{dD_{20}^2}{d\theta} = 11.65\times10^{-5}\left[2 + 0.35\left(\frac{D_{20}\Delta u \rho_a}{\mu_a}\right)^{0.6}\right]$$

Equation (17) gives Δu in terms of U_s and θ. By substituting this expression into the vaporization-rate equation,

$$\frac{dD_{20}^2}{d\theta} = 11.65\times10^{-5}\left[2 + 0.35\left(\frac{D_{20}U_s\rho_a}{\mu_a}\right)^{0.6} e^{-200\,\theta}\right] \qquad (25)$$

is obtained. This expression may be graphically integrated by taking small increments of θ and calculating the change in D_{20}^2.

It was found experimentally that the sprays had accelerated to approximately stream velocity in 0.014 second. Although D_{20}^2 decreased approximately 33 percent in this time, $D_{20}^{0.6}$ decreased only 5 percent. Thus, if $D_{20}^{0.6}$ is assumed approximately constant, the vaporization rate equation may be integrated to give

$$\Delta D_{20}^2 = 11.65\times10^{-5}\left\{0.028 + 1.75\times10^{-3}\left[\frac{(D_{20})_i U_s \rho_a}{\mu_a}\right]^{0.6}\right\}$$

since,

$$\int_{\theta=0}^{\theta=0.014} e^{-200\,\theta}\,d\theta = \frac{1 - e^{-200\,\theta}}{200} + C$$

where $C = 0.06$ for the condition of complete spray acceleration. By using the following values:

$(D_{20}^2)_i$, sq cm	2100×10^{-8}
U_s, ft/sec	140
μ_a, poises	1.8×10^{-4}
ρ_a, gm/cu cm	12.04×10^{-4}

the expression

$$\Delta D_{20}^2 = (326 + 375)\times10^{-8} = 701\times10^{-8} \text{ sq cm}$$

may be written. Graphical integration of equation (25) gave $D_{20}^2 = 700\times10^{-8}$ square centimeter (fig. 12) for $U_s = 140$ feet per second, and $\theta = 0.014$ second. Thus, a simple expression was obtained, since the change in the Reynolds number was controlled primarily by the change in velocity difference Δu and was affected very little by the change in D_{20}.

Calculation of weight percent evaporation during spray acceleration period. - The weight percent evaporated E during the spray acceleration period may be approximated by the expression

$$E = 100 \times \left\{1 - \left[(D_{20}^2)_f/(D_{20}^2)_i\right]^{1.5}\right\} \qquad (26)$$

since it was found experimentally that $D_{30}/D_{20} = 1.10\pm0.02$. Values of E calculated from this expression and experimental values of E are compared in the following table:

Air-stream velocity, U_s, ft/sec	Time, θ, sec	Distance from injector, x, in.	Evaporated portion of spray, E, percent	
			Experimental, from table III	Calculated from eq. (26)
140	0.011	14	40.0	44
180	0.011	18	51.2	51

Evaporation During Period Following Complete Spray Acceleration

The method of reference 7 may be used to calculate the weight percent evaporated after the spray has accelerated to stream velocity. In this method, the Rosin-Rammler expression (eq. (9)) is used. When the values of $\overline{D}$ and q are known, the weight percent unevaporated 100 - E may be determined.

The relation between $\overline{D}$ and D_{20} may be derived in the following manner: The Nukiyama-Tanasawa equation for mean drop sizes (ref. 11) predicts $D_{31}/D_{20} = 1.29$ which agreed within 2 percent of experimental values of D_{31}/D_{20} obtained in this investigation. Also, it was shown in reference 7 that the Rosin-Rammler expression for mean drop sizes gave $\overline{D} = \sqrt{2}\, D_{31}$ as a close approximation for $\overline{D}$ when $2 < n < 4$. Thus,

$$\overline{D} = 1.82\, D_{20}$$

may be written. Figure 12 shows $D_{20} = 43.6$ microns at $U_s = 140$ feet per second and $x = 5.5$ inches ($\theta = 0.0058$ sec). By substituting this value of D_{20} into the preceding expression, $\overline{D} = 79.5$ microns is obtained. This value agrees with figure 4 which shows $\overline{D} = 80$ microns. Experimental values of $\overline{D}/D_{20}$ agreed with the constant 1.82 within 2 percent.

In this study, the constant n in equation (9) was approximately 3 throughout the spray acceleration period. By using $n = 3$, and calculating $\overline{D}$ from the expression

$$\overline{D} = 1.82\left(\left(D_{20}^2\right)_i - 11.65\times10^{-5}\left\{0.028 + 1.75\times10^{-3}\left[\frac{(D_{20})_i U_s \rho_a}{\mu_a}\right]\right\}^{0.6}\right)^{0.5}$$

The weight percent evaporated E following the acceleration period may be determined from the plot of reference 7 of 100 - E against $\sqrt{\lambda\theta}/\overline{D}$ (where $\lambda = 23.3\ 10^{-5}$ cm^2/sec and θ is the time following the spray acceleration period). Thus, the total weight percent evaporated may be calculated as the percent evaporated during the spray acceleration period

plus the weight percent of the remaining fraction evaporated in the final evaporation period.

Application of Method of Reference 7 to Spray Acceleration Period

If it were assumed that the spray traveled at stream velocity ($\Delta u = 0$ and $Nu = 2$) in the 140-foot-per-second air stream for the distance $x = 18$ inches ($\theta = 0.014$ sec), the weight percent evaporated would be calculated in the following manner: From the plot of reference 7 of weight percent unevaporated spray (100 - E) against $\sqrt{\lambda\theta/D}$, the expression

$$\sqrt{\lambda\theta/D} = \frac{23.3\times10^{-5} \times 0.014}{83.5\times10^{-4}} = 0.198$$

may be obtained, from which $100 - E = 88$ percent, or $E = 12$ percent evaporated. This value of E is approximately 30 percent less than the experimental value given in table III. Thus, a very serious error would be made if the evaporation of the spray during the acceleration period was assumed the same as evaporation in a quiescent atmosphere.

REFERENCES

1. Lee, Dana W.: Effect of Nozzle Design and Operating Conditions on the Atomization of Fuel Sprays. NACA Rep. 425, 1932.

2. Houghton, H. G.: Spray Nozzles. Chemical Engineers' Handbook, John H. Perry, ed. Third ed., McGraw-Hill Book Co., Inc., 1950, pp. 1170-1175.

3. Longwell, John P., and Weiss, Malcolm A.: Mixing and Distribution of Liquids in High-Velocity Air Streams. Ind. and Eng. Chem., vol. 45, no. 3, Mar. 1953, pp. 667-677.

4. Bahr, Donald W.: Evaporation and Spreading of Isooctane Sprays in High-Velocity Air Stream. NACA RM E53I14, 1953.

5. Ingebo, Robert D.: Vaporization Rates and Heat-Transfer Coefficients for Pure-Liquid Drops. NACA TN 2368, 1951.

6. Ingebo, Robert D.: Study of Pressure Effects on Vaporization Rate of Drops in Gas Streams. NACA TN 2850, 1953.

7. Probert, R. P.: The Influence of Spray Particle Size and Distribution in the Combustion of Oil Droplets. Phil. Mag., ser. 7, vol. 37, no. 265, Feb. 1946, pp. 94-105.

8. McCullough, Stuart, and Perkins, Porter J.: Flight Camera for Photographing Cloud Droplets in Natural Suspension in the Atmosphere. NACA RM E50K01a, 1951.

9. Bevans, Rowland S.: Mathematical Expressions for Drop Size Distribution in Sprays. Conf. on Fuel Sprays, Univ. of Michigan, Mar. 30-31, 1949.

10. Nukiyama, Shirō, and Tanasawa, Yasushi (E. Hope, Trans.): Experiments on the Atomization of Liquids in an Air Stream. Rep. No. 3, On the Droplet-Size Distribution in an Atomized Jet, Defence Res. Board, Dept. Nat. Defence, Ottawa (Canada), Mar. 18, 1950. (Trans. from Trans. Soc. Mech. Eng. (Japan), vol. 5, no. 18, Feb. 1939, pp. 62-67.)

11. Mugele, R. A., and Evans, H. D.: Droplet Size Distribution in Sprays. Ind. and Eng. Chem., vol. 43, no. 6, June 1951, p. 1317.

12. Perry, John H., ed.: Chemical Engineers' Handbook. Third ed., McGraw-Hill Book Co., Inc., 1950.

13. Lane, W. R.: Shatter of Drops in Streams of Air. Ind. and Eng. Chem., vol. 43, no. 6, June 1951, pp. 1312-1317.

14. Hinze, J. O.: Critical Speeds and Sizes of Liquid Globules. Appl. Sci. Res., vol. A, 1949, pp. 273-288.

TABLE I. - DROP-SIZE-DISTRIBUTION DATA FOR SEVEN-POINT TRAVERSE OF SPRAY CROSS SECTION

[Air-stream velocity, U_s, 140 ft/sec; distance from injector orifice, x, 18 in.]

Drop-diameter, D, microns		Number of drops, n									
		Traverse position[b]							Total for first traverse	Second traverse	Total for two traverses
Range[a]	Average	1	2	3	4	5	6	7			
0- 4.8	2.5	0	0	0	1	2	1	2	6	4	10
4.8- 9.5	7.0	0	2	1	5	2	5	3	18	15	33
9.5- 14.3	12.0	3	6	0	8	7	10	8	42	54	96
14.3- 19.0	17.0	9	11	6	13	8	16	10	73	56	129
19.0- 23.8	21.5	13	27	29	31	12	24	16	152	103	255
23.8- 28.5	26.0	16	18	14	19	15	30	20	132	82	214
28.5- 33.3	31.0	18	6	24	9	17	17	17	108	78	186
33.3- 38.0	36.0	15	11	14	11	15	8	17	91	36	127
38.0- 42.8	40.5	14	10	17	4	9	8	10	72	29	101
42.8- 47.5	45.0	7	11	9	5	4	2	8	46	24	70
47.5- 52.3	50.0	3	4	4	4	5	3	7	30	21	51
52.3- 57.0	55.0	5	6	4	3	9	1	3	31	13	44
57.0- 61.8	59.5	2	2	1	2	4	1	4	16	20	36
61.8- 66.5	64.0	9	2	1	3	4	1	3	23	6	29
66.5- 71.3	69.0	6	4	2	3	5	0	1	21	6	27
71.3- 76.0	74.0	5	2	0	2	0	0	0	9	10	19
76.0- 80.8	78.5	1	1	2	3	3	2	1	13	0	13
80.8- 85.5	83.0	1	0	1	3	2	0	0	7	2	9
85.5- 90.3	88.0	2	2	1	0	3	0	0	8	1	9
90.3- 95.0	93.0	0	2	0	0	3	0	0	5	3	8
95.0- 99.8	97.5	0	0	0	1	0	1	0	2	1	3
99.8-104.5	102.0	0	1	0	0	1	0	0	2	0	2
104.5-109.3	107.0	0	1	0	0	0	0	0	1	0	1
109.3-114.0	112.0	0	1	0	0	0	0	0	1	0	1
	Total	129	130	130	130	130	130	130	909	564	1473

[a] ΔD = 4.75 microns.

[b] Fig. 1.

CA-4

TABLE II. - SUMMARY OF DROP-SIZE-DISTRIBUTION DATA

Average drop diameter, D, microns	Air-stream velocity, U_s, ft/sec							
	140				180			
	Distance from injector, x, in.							
	1	5.5	14	18	1	5.5	14	18
	Number of drops, n							
2.5	8	12	10	10	16	20	23	26
7	24	37	36	33	30	49	65	54
12	51	76	78	96	66	66	102	111
17	76	120	148	129	86	103	183	188
21.5	115	176	194	255	132	168	237	234
26	155	200	229	214	165	189	304	241
31	187	260	201	186	241	239	298	233
36	234	267	153	127	241	190	221	158
40.5	144	172	115	101	148	136	157	122
45	127	123	85	70	125	100	114	81
50	100	72	70	51	84	73	60	66
55	93	68	57	44	73	60	51	53
59.5	74	60	37	36	57	38	36	28
64	53	40	30	29	44	25	25	25
69	44	36	20	27	25	20	17	12
74	33	23	17	19	18	15	11	12
78.5	31	19	13	13	11	10	8	5
83	24	17	13	9	12	7	4	5
88	14	13	11	9	8	3	4	3
93	9	8	4	8	6	3	3	1
97.5	4	5	5	3	4	1	1	-
102	5	4	2	2	3	2	2	-
107	3	3	2	1	1	1	-	-
112	1	3	1	1	1	1	-	-
116.5	1	2	-	-	-	-	-	-
121	0	2	-	-	-	-	-	-
126	1	1	-	-	-	-	-	-
Total	1611	1819	1531	1473	1597	1519	1926	1658

TABLE III. - WEIGHT PERCENT OF SPRAY EVAPORATED

Distance from injector, x, in.	$D_{30}^3 \times 10^{10}$, cc	Weight percent evaporated	
		Experimental	Calculated from equation (23)
Air-stream velocity, U_s, 140 ft/sec			
0	[a]1279	----	0
1	1182	7.6	7.0
5.5	952	25.6	24.1
14	768	40.0	41.0
18	738	42.3	46.5
Air-stream velocity, U_s, 180 ft/sec			
0	[a]1036	----	0
1	863	16.7	8.9
5.5	692	33.2	28.0
14	537	48.3	46.0
18	506	51.2	51.5

[a]Calculated from $D_{30}/D_{20} = 1.10$ where D_{20} was obtained from fig. 12 at $x = 0$.

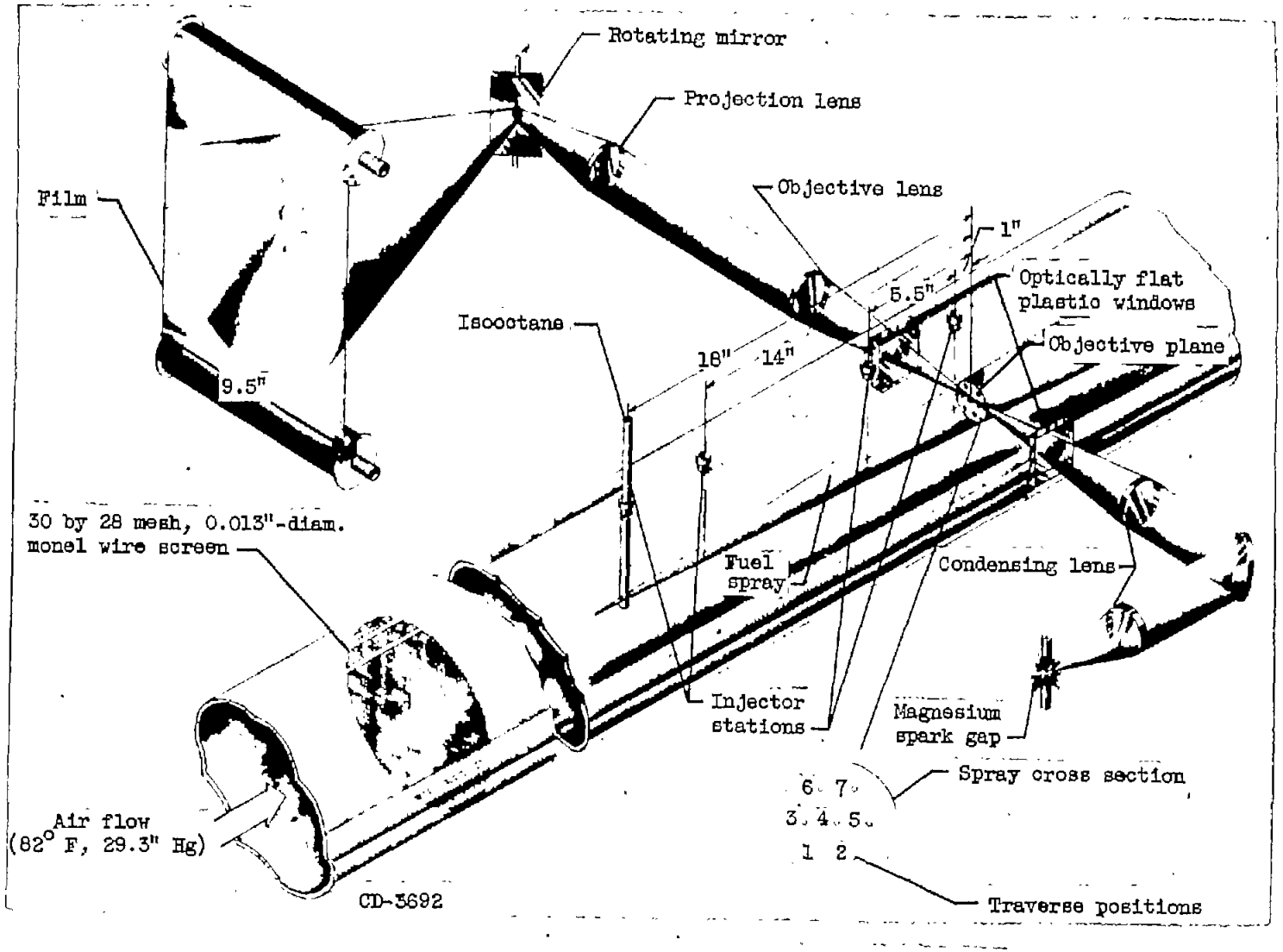

Figure 1. - Schematic diagram of test section and camera unit.

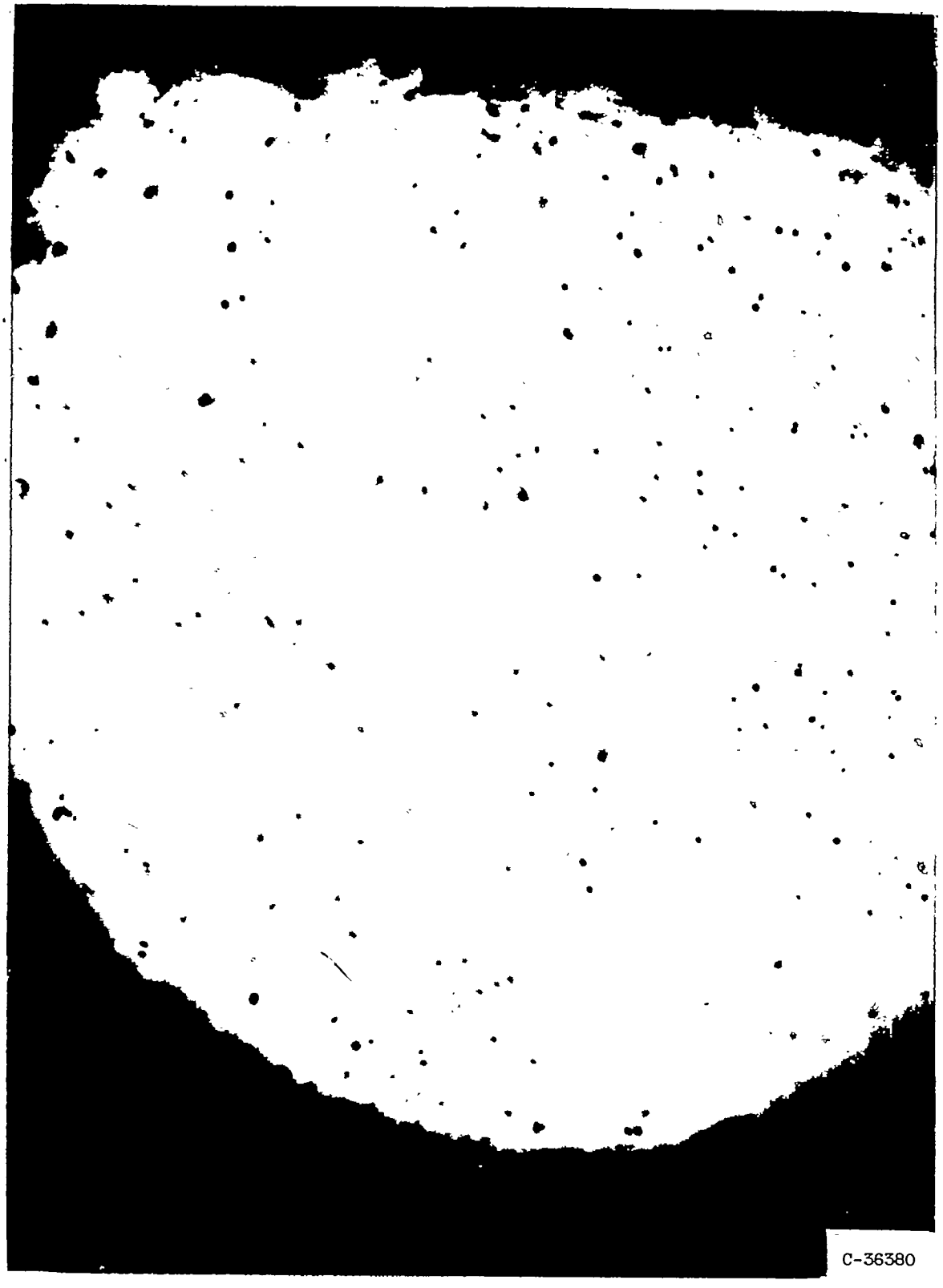

Figure 2. - Photomicrograph of isooctane spray in 180-foot-per-second air stream.

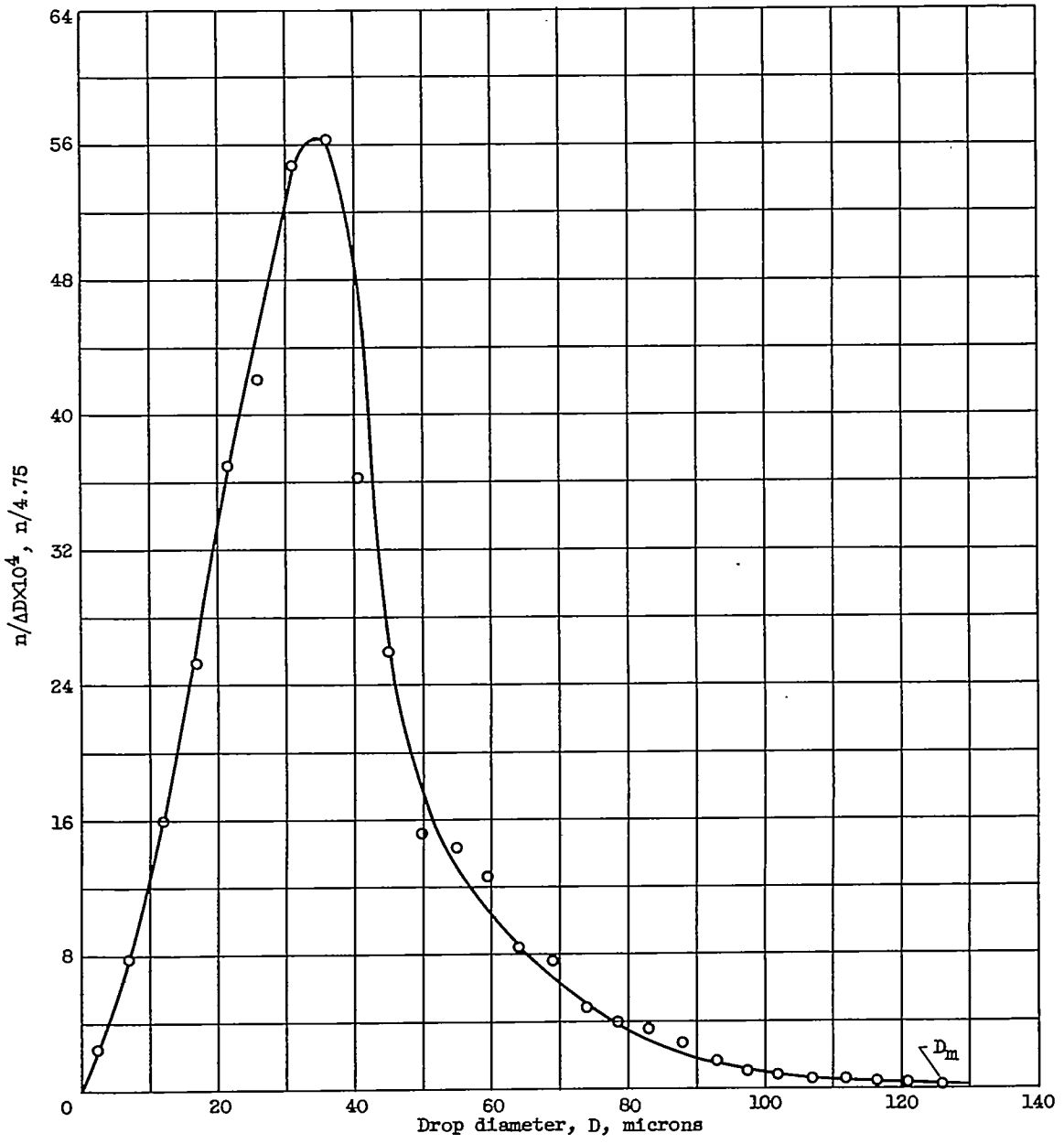

Figure 3. - Droplet-size distribution. Air-stream velocity, 140 feet per second; distance from injector, 5.5 inches.

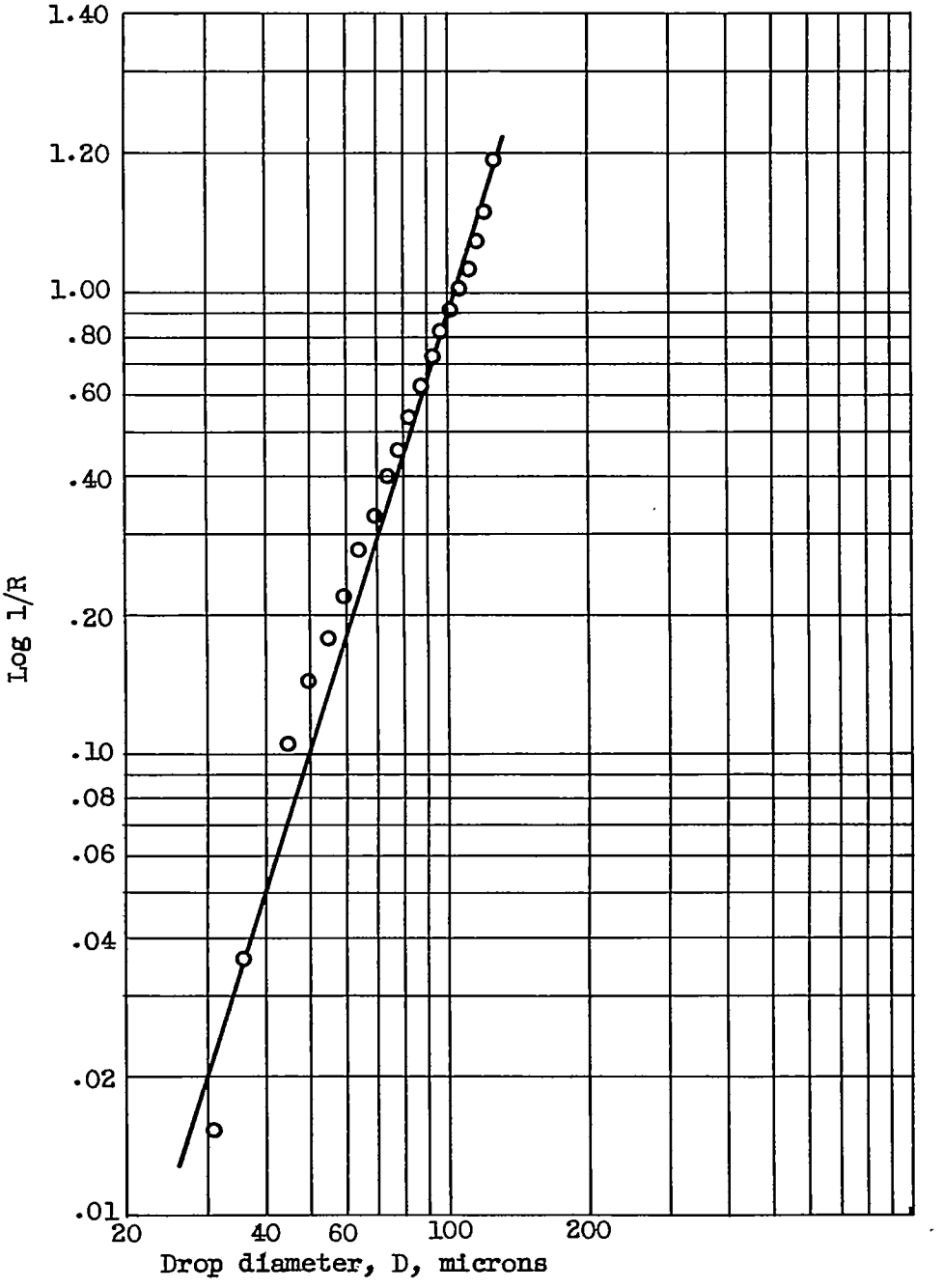

Figure 4. - Rosin and Rammler analysis. Air-stream velocity, 140 feet per second; distance from injector, 5.5 inches; $\overline{D}$, 80 microns; mean drop diameter D_{20}, 21.1 microns; q, 3.1.

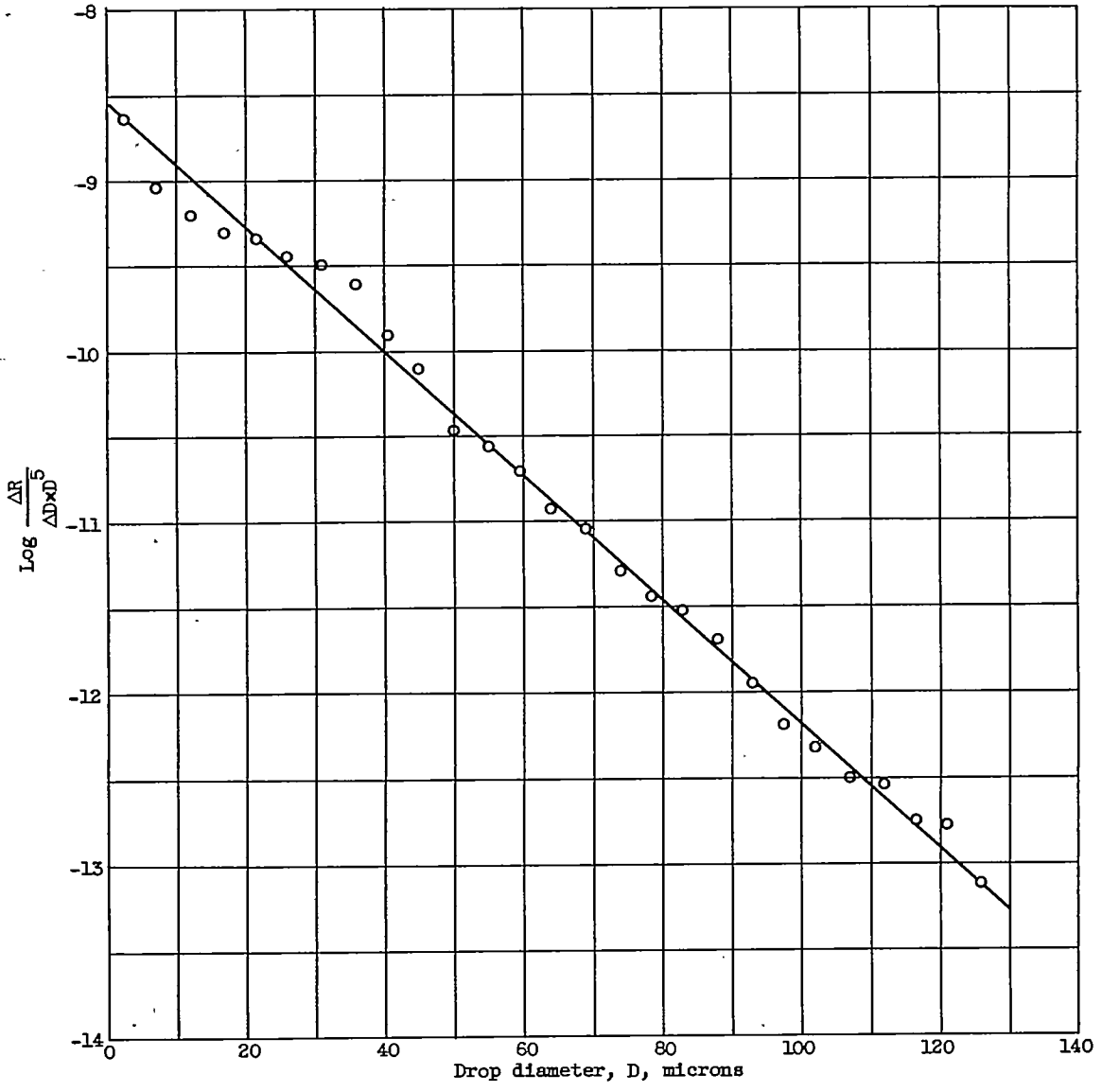

Figure 5. - Nukiyama and Tanasawa analysis. Air-stream velocity, 140 feet per second; distance from injector, 5.5 inches; mean drop diameter D_{20} 41.3 microns; b, 0.0837.

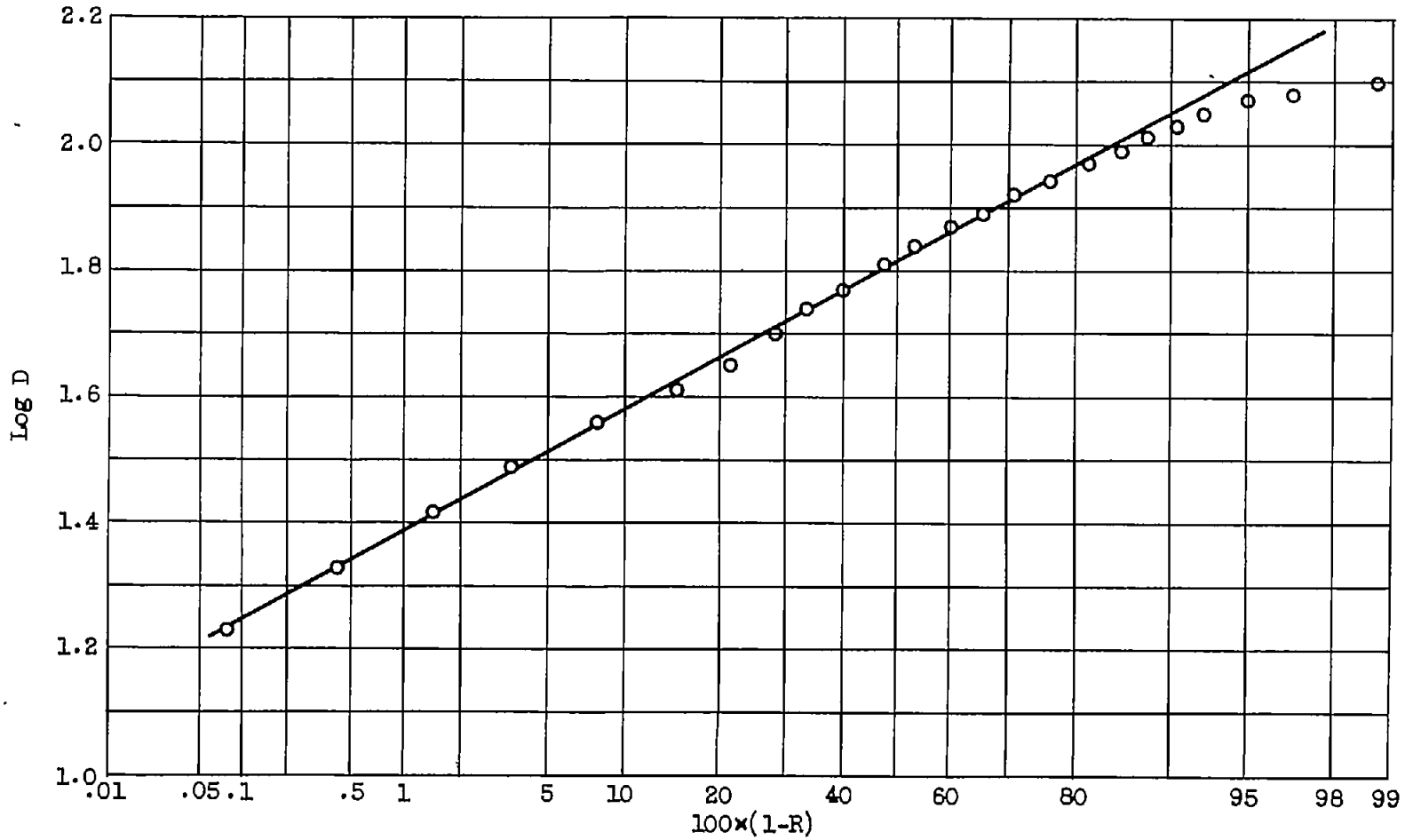

Figure 6. - Log-probability analysis. Air-stream velocity, 140 feet per second; distance from injector, 5.5 inches; D, 66 microns; δ, 1.712; mean drop diameter D_{20}, 40.7 microns.

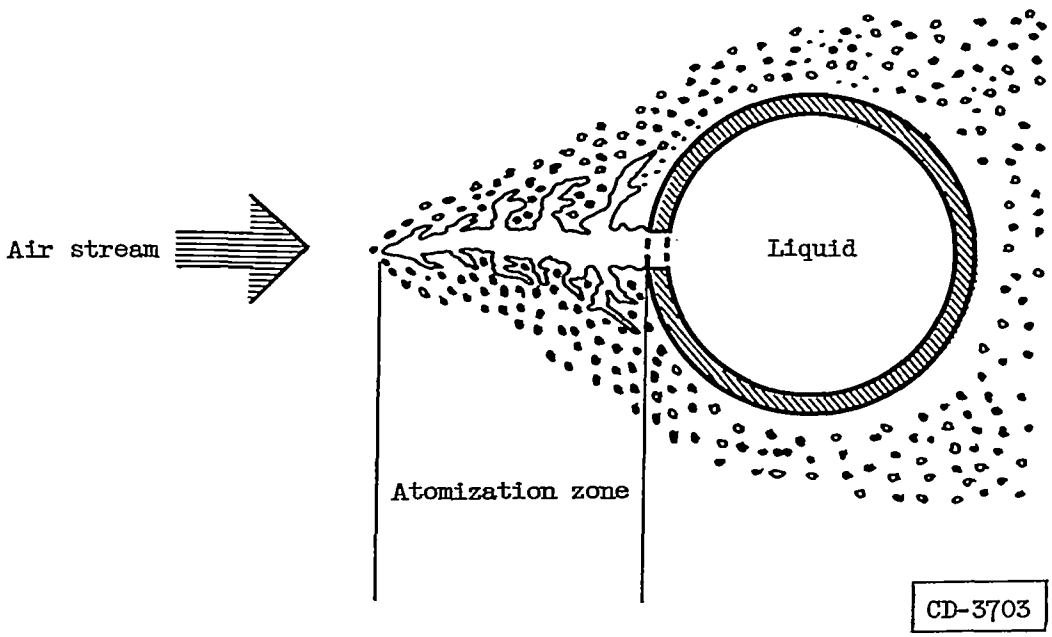

Figure 7. - Break-up of liquid fuel jet in turbulent air stream.

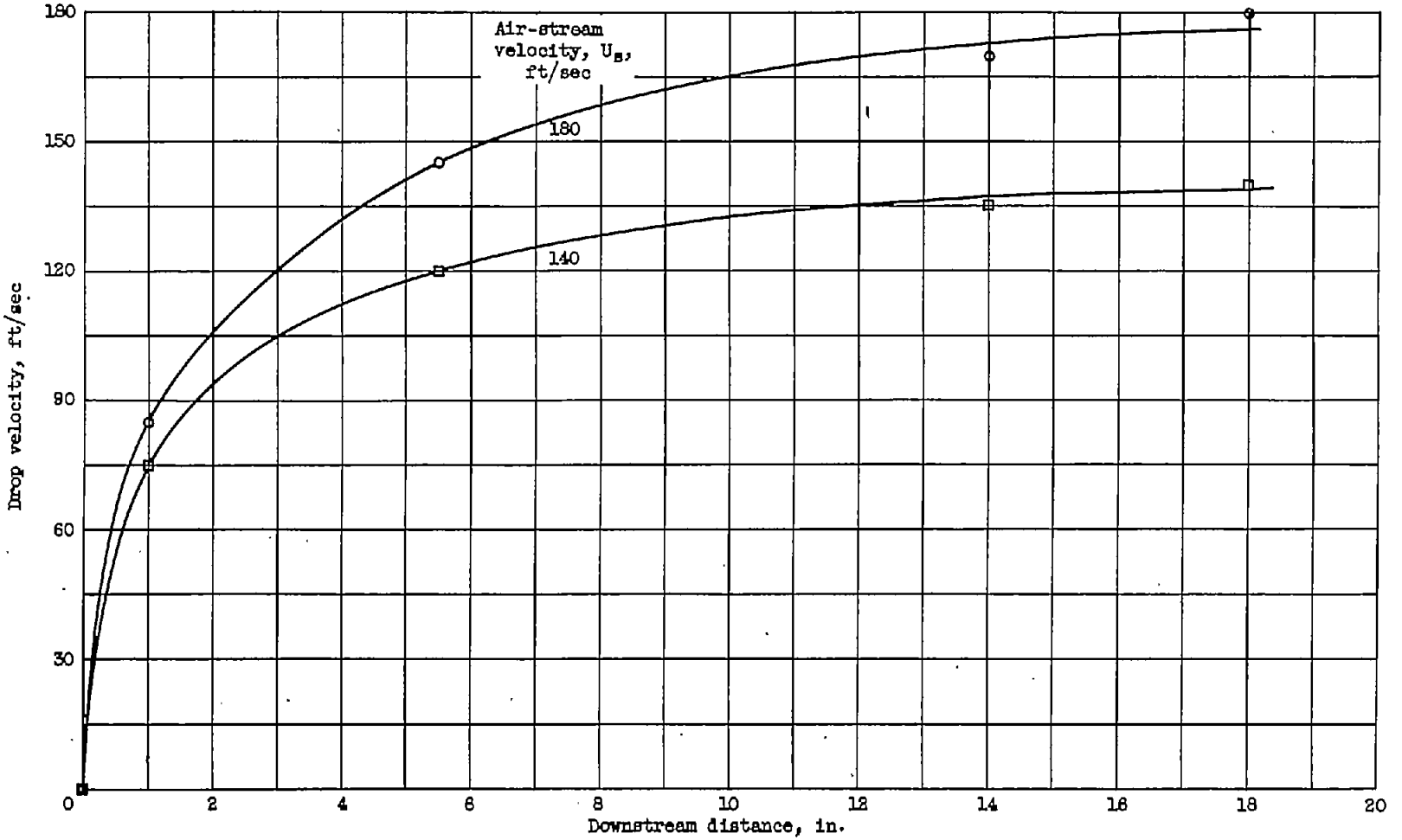

Figure 8. - Velocity of isooctane droplets at given distances downstream of fuel-injector orifice.

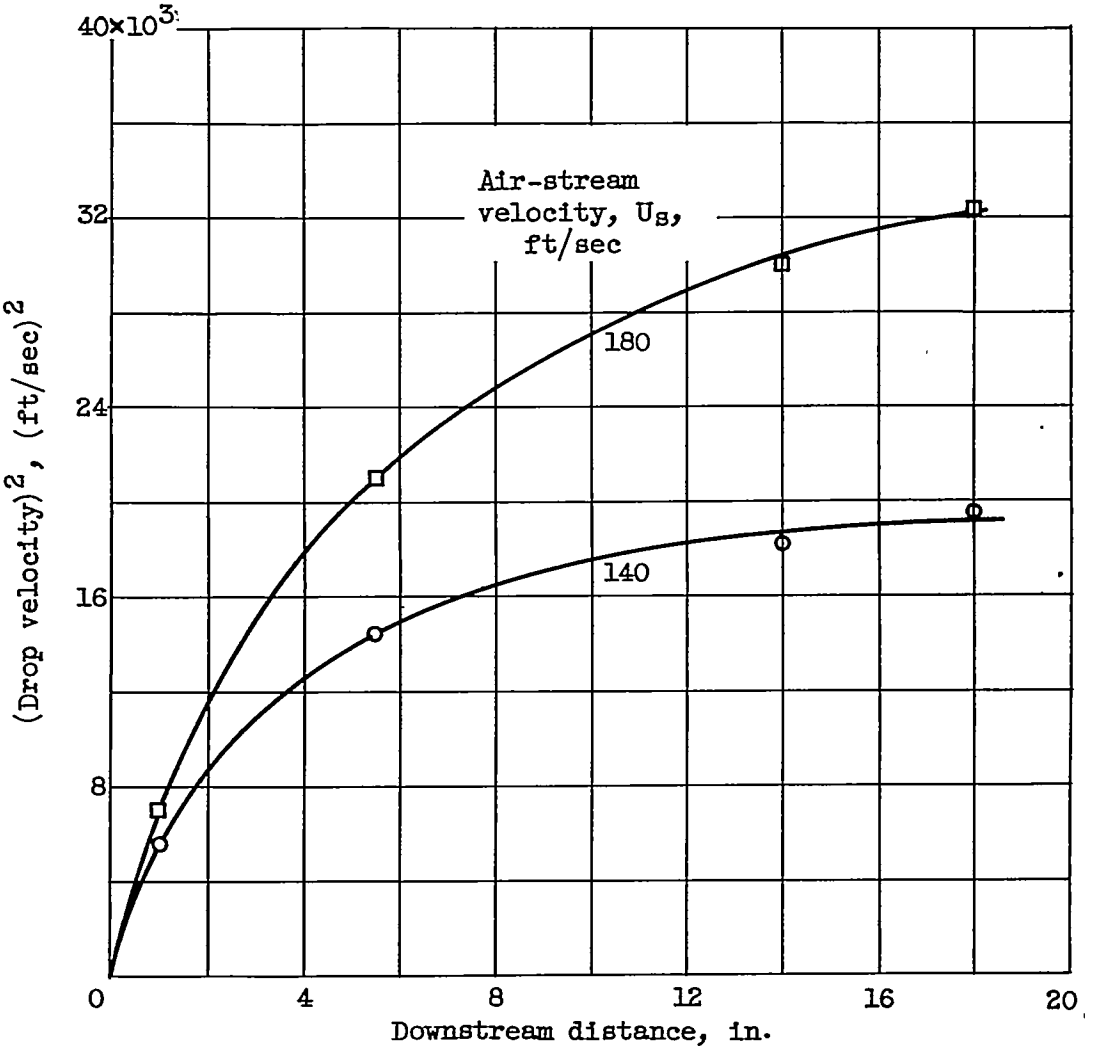

Figure 9. - Acceleration of isooctane droplets.

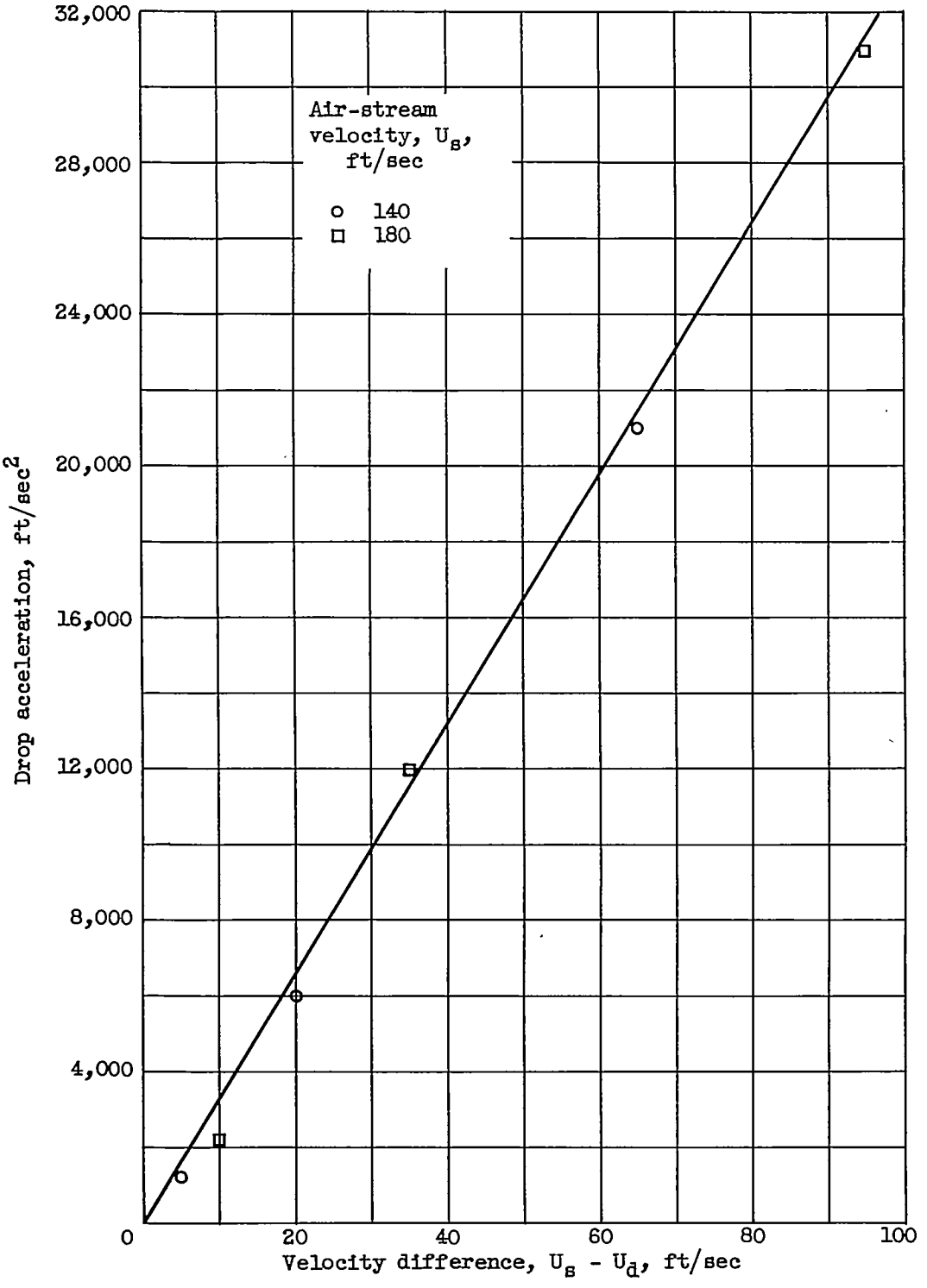

Figure 10. - Relation between drop acceleration and velocity difference.